Turkish Journal of Chemistry

http://journals.tubitak.gov.tr/chem/

Research Article

Turk J Chem
(2019) 43: 213 – 228

doi:10.3906/kim-1803-49

In situ preparation of hydroxyapatite composites into hydrolyzed polyacrylamide solution and methylene blue dye retention

Ali MANSRI[1], **Hanane MAHROUG**[1,*], **Fayçal DERGAL**[1,2]

[1]Laboratory of Organic Electrolytes and Polyelectrolytes' Application, Department of Chemistry, Faculty of Science, University of Tlemcen, Tlemcen, Algeria

[2]Scientific Research Center of Techniques in Physicochemical Analysis, Tipaza, Algeria

Received: 18.03.2018 • **Accepted/Published Online:** 17.11.2018 • **Final Version:** 05.02.2019

Abstract: Four composites of hydroxyapatite/hydrolyzed polyacrylamide (HAP/HPAM-n) were prepared using an in situ wet chemical method. The synthesis was performed by preparing a suspension of calcium in a copolymer solution having a known HPAM concentration. Phosphoric acid was added dropwise to each suspension to obtain HAP/HPAM-n composites. The effect of initial copolymer amount on the composite properties was investigated using XRD, FTIR, TGA, and SEM/EDS analysis. The obtained results were compared to the HAP sample synthesized under the same conditions and without copolymer. HPAM amount in the composite affects the retention of methylene blue (MB) dye. The result shows that the increase of HPAM in the material leads to the increase of the dye retention capacity. Therefore, the composite prepared with a higher copolymer amount was selected to study the effects of different parameters on the dye removal including contact time, concentration, pH, temperature, and composite regenerations. We deduce in this work that the composite HAP/HPAM-75 is a good candidate for MB dye retention from aqueous solution with a maximum removal capacity of 435.6 mg g^{-1} and the possibility of its reuse for several times.

Key words: Hydroxyapatite, hydrolyzed polyacrylamide, in situ preparation, methylene blue, retention

1. Introduction

$Ca_{10}(PO_4)_6(OH)_2$ is the chemical formula of hydroxyapatite (HAP), whose importance is explained by its similarity to the mineral part of bone and tooth and its utilization in medicine and dentistry fields.[1,2]

HAP has good thermal and adsorption properties and high exchangeability with metals. It is used, the last decades, in many industrial and technological applications and as a good electrolyte in fuel cells.[3] It is also used in column chromatography[4,5] and largely studied to remove heavy metals and organic pollutants from wastewaters and soils.[6–9]

In the majority of its applications, HAP is combined with other molecules or macromolecules. Thus, many synthetic routes are described in the literature to obtain composites based on HAP. Hakimimehr et al.[9] prepared HAP by an in situ method using poly(propylene fumarate) as a soluble polymer. El-Hag Ali[10] reported the in situ synthesis of nanohydroxyapatite within gelatin/acrylic acid copolymer hydrogels using γ-radiation induced copolymerization and cross-linking. Syusyukina et al.[11] reported the preparation of composite materials based on polylactide and HAP using already prepared HAP and polymer.

In this work, for the first time, we use already prepared hydrolyzed polyacrylamide (HPAM) with

*Correspondence: hadjar_hanen@hotmail.fr

high molecular weight to obtain HAP/HPAM-n composites. In fact, the majority of literature works use the acrylamide monomer, which is polymerized into HAP or simultaneously with HAP formation in the presence of N,N'-methylene bis-acrylamide as a cross-linker.[12,13] We are using 27% HPAM, which is water-soluble and carries negative charges along its repeating units. Thus, different HAP/HPAM-n properties and structures were obtained by the in situ preparation method. The method used leads to formation of HAP particles in the HPAM copolymer medium. Thus, four composites containing different copolymer amounts of 0.75%, 3%, 30%, and 75% were prepared and characterized by several techniques.

Although different materials have been used for methylene blue (MB) dye retention,[14–16] the composites prepared here have never been used for this purpose. In fact, the initial copolymer amount affects the MB dye removal. Therefore, we selected the material with the best retention power to determine the kinetics, isotherms, thermodynamic parameters, and material reuse for the dye retention.

2. Results and discussion

2.1. Sample formation

Two series of HAP/HPAM-n composites were prepared by successively adding calcium ions and phosphoric acid to HPAM copolymer. The first series was prepared using low amounts of HPAM (n = 0.75 and n = 3) and the second series was prepared with a significant amount of HPAM (n = 30 and n = 75). The mechanism of material formation is represented in Figure 1.

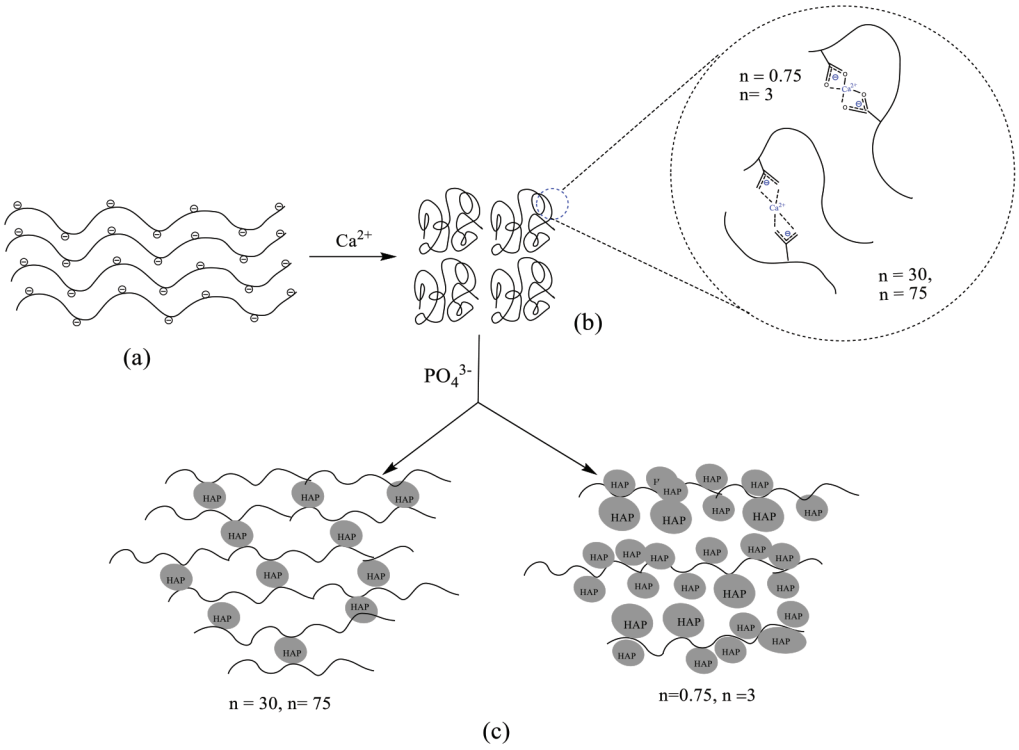

Figure 1. Formation mechanism of HAP/HPAM-n composites: (a) extended HPAM chains, (b) calcium ions' addition, and (c) phosphate ions' addition.

The preparation of HAP/HPAM-n materials was started by preparing a solution of HPAM with the

desired concentration in order to obtain the required copolymer amount in each composite. The viscosity of the HPAM solutions used for preparing the second series of composites is very important. The importance of viscosity can be explained by the nature of the copolymer that contains carboxylate functions among its repeated units and behaves as a negatively charged polyelectrolyte in aqueous solution. The presence of the negative charges causes the electrostatic repulsion forces in HPAM chains, leading to extended backbones, i.e. high viscosity (Figure 1a).

When calcium ions were added as a divalent metal to the HPAM solution, they formed a cross-link through complex formation with carboxylate groups of the copolymer backbone as seen in Figure 1a. Similar behavior was obtained with biopolymers such as sodium alginate and pectin, which have carboxyl groups on the polymer chains, and the chains of these polymers can be cross-linked with divalent or trivalent ions, e.g., Ca^{2+} and Al^{3+}.[17–19]

On the other hand, Wang et al.[20] reported that the complex formed between Ca^{2+} and negatively charged poly(vinyl phosphonic acid-co-acrylic acid) depends on the calcium concentration. Wang et al.[20] also reported that a complex interpolymer can be formed when the calcium concentration is important.

In the same way, we proposed the formation of the complex HPAM-Ca at low HPAM concentration (n = 0.75 and n = 3) and the complex HPAM-Ca-HPAM at high HPAM concentrations (n = 30 and n = 75) (Figure 1b). Hence, carboxylate groups are considered as sites of HAP formation and growth leading to HAP phase was linked to the HPAM copolymer.

Moreover, a significant decrease in the viscosity of HPAM solutions was observed after calcium addition. We explain this phenomenon by a change in the copolymer conformation, from extended chains to random coil conformations, because of the screening of the negative charges of HPAM with the calcium ions. The screening charge in the partially hydrolyzed polyacrylamide with monovalent cations and its interaction with P4VP and DPC was reported by Mansri et al.[21,22]

The last step for HAP/HPAM-n formation is phosphoric acid (H_3PO_4) addition. By adding H_3PO_4, the two series of HAP/HPAM-n were obtained according to Figure 1c. The use of high copolymer concentration (n = 30 and n = 75) leads to a network of copolymer chains related to HAP particles with remarkable swelling properties in water. After the formation of HAP/HPAM-n, the materials were washed with double distilled water in order to remove all unreacted starting materials. After that, the materials were dried in an oven at 70 °C for 12 h.

After obtaining the final materials, a reaction occurred with the preparation of a suspension of HAP/HPAM-30 and HAP/HPAM-75 in double distilled water with the concentration 10 g L^{-1}. After 48 h of agitation at 400 rpm, the supernatant was analyzed by UV-Vis method by measuring its absorbance at the maximal absorption wavelength of HPAM at 196 nm. The obtained results prove that any absorbance was recorded at 196 nm, indicating that no HPAM is released in solution.

2.2. Evaluation of composite structure and properties

2.2.1. XRD

Figures 2a–2d represent the XRD patterns of HAP, HAP/HPAM-0.75, HAP/HPAM-3, and HAP/HPAM-30, respectively. The diffractograms were compared with PDF card no. 01-072-9863. Their relative patterns present all diffraction peaks of the carbonated HAP structure $Ca_{10}(PO_4)_{5.64}(CO_3)_{0.66}(OH)_{3.03}$, without any other phase of calcium phosphate. Thus, the Ca/P ratio in the mentioned formula is 1.77.

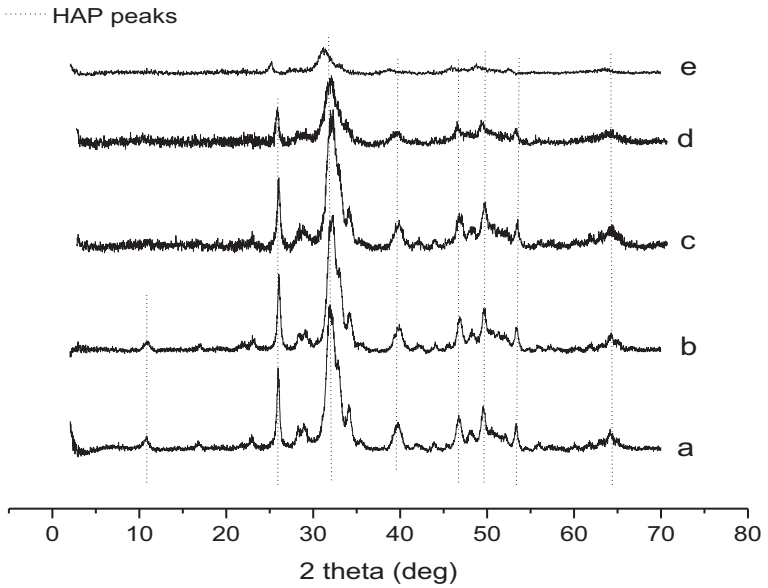

Figure 2. XRD patterns of (a) HAP, (b) HAP/HPAM-0.75, (c) HAP/HPAM-3, (d) HAP/HPAM-30, and (e) HAP/HPAM-75 with $2\theta = 0.02°$.

The HAP/HPAM-75 diffractogram is presented in Figure 2e. Its mineral part is defined by PDF card no. 01-073-8421 corresponding to the formula $Ca_5(PO_4)_3(OH)$ with Ca/P ratio equal to 1.67.

The patterns also show a decrease of peak intensities due to the decrease in HAP amount contained in the powders when HPAM amount increases. The formation of carbonated HAP with the structure $Ca_{10}(PO_4)_{5.64}(CO_3)_{0.66}(OH)_{3.03}$ is explained by the medium alkalinity leading to dissociate released CO_2 to CO_3^{2-} during the synthesis and its reaction with calcium as a bivalent ion. Effects of HPAM on the lattice crystal properties of unit cell parameters (a, b, and c), cell volume (V), and density (d) of composites are presented in Table 1. We observe that (a) and (c) unit cell parameters of HAP in all the prepared materials increase with increasing HPAM percentages from 0.75% to 30%. The same observation is made for the cell unit volume. This is accompanied by a decrease in the composite densities reported in the Table 1. These results can be explained by the linkage of the copolymer carboxylate groups in the HAP-HPAM composites. Hydrolyzed functions are considered as a nucleation center of crystal formation and growth. The most important result from XRD analysis is that HPAM cannot inhibit HAP formation and the crystallites were formed within the copolymer. This was not observed with other polymers such as poly(propylene fumarate) when only amorphous calcium phosphate was formed.[9]

Table 1. Cell unit parameters (a, b, c), volume crystalline (V), and density (d) of HAP and HAP/HPAM-n composites.

	a = b (Å)	c (Å)	V (Å^3)	d
HAP	9.4256	6.8663	528.2938	3.230
HAP/HPAM-0.75	9.3770	6.8582	522.2451	3.274
HAP/HPAM-3	9.5335	7.0088	551.6787	3.099
HAP/HPAM-30	9.7016	7.0567	575.2180	2.900
HAP/HPAM-75	9.7153	7.0446	575.8412	2.897

2.2.2. FTIR

In Figure 3a, the FTIR spectrum of HAP confirms its formation by the bands at 1100 cm^{-1} and 575 cm^{-1} assigned to the phosphate groups.[23,24] In Figure 3b, the HPAM spectrum also shows strong stretching vibration peaks at 3400 cm^{-1} and 1662 cm^{-1}, attributed respectively to the amino and carbonyl groups of the amides.[25] The absorption band at 1400 cm^{-1} is due to C–N stretching.[26]. The bands at 2924 cm^{-1} and 2853 cm^{-1} are attributed to the hydroxyl groups in the HPAM.

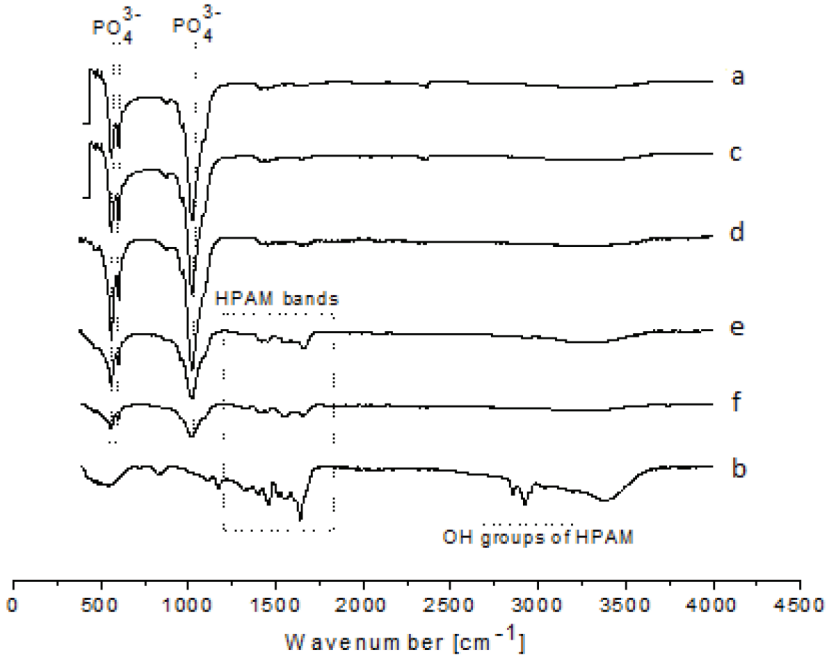

Figure 3. FTIR spectra of (a) HAP, (b) HPAM, (c) HAP/HPAM-0.75, (d) HAP/HPAM-3, (e) HAP/HPAM-30, and (f) HAP/HPAM-75.

Figures 3c and 3d correspond to the materials HAP/HPAM-0.75 and HAP/HPAM-3, respectively. The comparison of these figures with Figures 3a and 3b corresponding to HAP and HPAM, respectively, shows only the bands attributed to the HAP. On the other hand, HAP bands are also visible in HAP/HPAM-30 and HAP/HPAM-75, but with low intensities according to Figures 3e and 3f. High HPAM percentage is presented in these last two composites and makes the copolymer bands visible. Another interesting observation is seen in Figure 3. The bands at 2924 cm^{-1} and 2853 cm^{-1} are attributed to the hydroxyl group in HPAM alone and do not exist in the composites, including composites prepared with high HPAM amount. This result confirms that the hydrolyzed OH is completely linked to the HAP phase. We can conclude that the negative charges created in alkaline medium are sites of HAP nucleation and growth. In the same way, we observe that OH groups also disappear from FTIR spectra, confirming that they transform to hydrolyzed OH following the proposed mechanism represented in Figure 1.

2.2.3. TGA

The TGA curves for HAP, HPAM, and HAP/HPAM-n composites are presented in Figure 4. The weight loss observed in the HAP reference sample shown in Figure 4a is attributed to the adsorbed and confined water molecules up to 350 °C. At higher temperatures, the weight loss corresponds to the dehydration and

decarbonation of the mineral structure. According to Figures 4b and 4c, materials HAP/HPAM-0.75 and HAP/HPAM-3 present similar thermal behavior as HAP material, because of the lower copolymer amount in the composites. The HAP/HPAM-30 and HAP/HPAM-75 thermograms given by Figures 4d and 4e are also similar to HAP in the temperature range from 50 °C to 200 °C. In Figure 4f, the HPAM thermal behavior presents three principal ranges. The first range until 200 °C corresponds to 12% of weight loss of all small molecules adsorbed by the copolymer chains. Between 200 °C and 589 °C, the copolymer chains show a weight loss of 64.84%. The last range of HPAM degradation is characterized by a residual mass of 23.16%. The HPAM contained in the composites is degraded in the range between 250 °C and 589 °C. From 589 °C, the composites HAP/HPAM-30 and HAP/HPAM-75 also have an important weight loss of 5.69% and 6.73%, respectively, which is due to the carbonate leaving both mineral and organic phases.

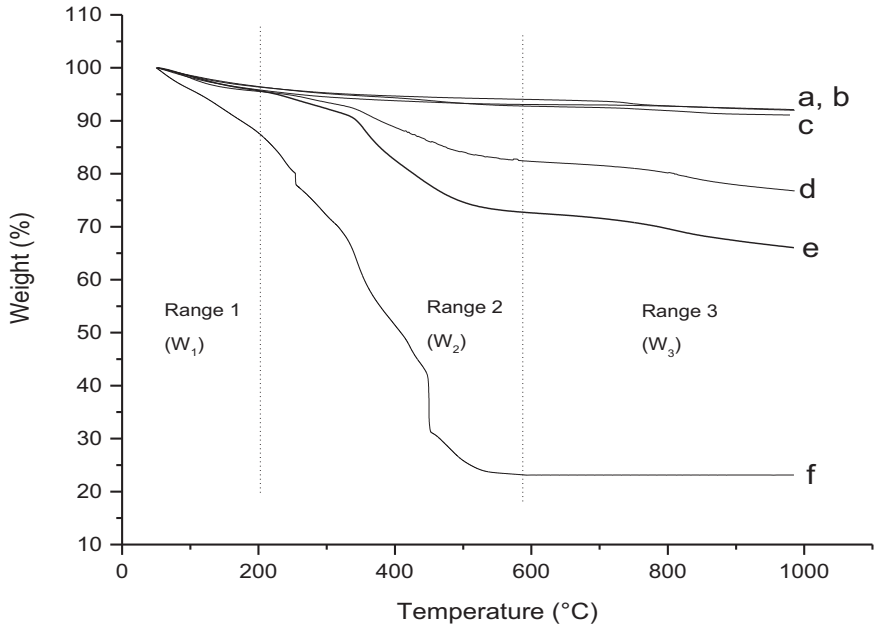

Figure 4. TGA thermograms of (a) HAP, (b) HAP/HPAM-0.75, (c) HAP/HPAM-3, (d) HAP/HPAM-30, (e) HAP/HPAM-75, and (f) HPAM.

Table 2 presents the weight loss percentage in each range (W_1, W_2, W_3), the total weight loss (W_t), the weight loss corresponding to the HPAM degradation in composites (W_d) calculated by subtracting composites' total weight loss, and HAP total weight loss. Table 2 also presents the final copolymer percentage in the composites ($W_{p,f}$) calculated by the following equation:

$$W_{p,f}(\%) = W_d(1 + 23.16/100). \quad (1)$$

From Table 2, we also observe that the fixed percentage of HPAM in the composite is important and it is more than 75% for HAP/HPAM-30 and HAP/HPAM-75. For HAP/HPAM-0.75, the determination of the final copolymer percentage is not possible by the TGA method because of the small amount of the copolymer.

2.2.4. SEM/EDS

The synthesized powders differ by their composition and crystalline form and also by their morphology according to Figures 5a–5e, where different morphologies are represented. Figure 5a shows that the HAP surface is

Table 2. Determination of the weight loss due to HPAM degradation (W_d), the final HPAM percentage ($W_{p,f}$), and the fixed percentage compared to the initial percentage of HPAM (P_{fix}), from the weight losses in the range of 50–200 °C (W_1), 200–589 °C (W_2), 589–1000 °C (W_3) and the total weight loss (W_t) in each powder.

	W_t	W_1	W_2	W_3	W_d (%)	$W_{f,p}$ (%)	P_{fix} (%)
HAP	7.89	3.57	2.29	2.03	0	0	/
HAP/HPAM-0.75	7.84	4.08	2.78	0.98	/	/	/
HAP/HPAM-3	8.9	3.57	3.65	1.68	1.01	1.36	46.82
HAP/HPAM-30	23.23	4.29	13.25	5.69	15.34	18.90	82.20
HAP/HPAM-75	33.95	4.29	22.93	6.73	26.06	32.11	75.14
HPAM	76.84	12	64.84	0	/	/	/

characterized by different aggregations with sizes until 4 µm. The powders prepared from the copolymer show that the surfaces are recovered with HPAM, especially as observed in HAP/HPAM-3 (Figure 5c) and HAP/HPAM-30 (Figure 5d). HAP/HPAM-75 is obviously a highly porous composite with interconnected pores according to the Figure 5e.

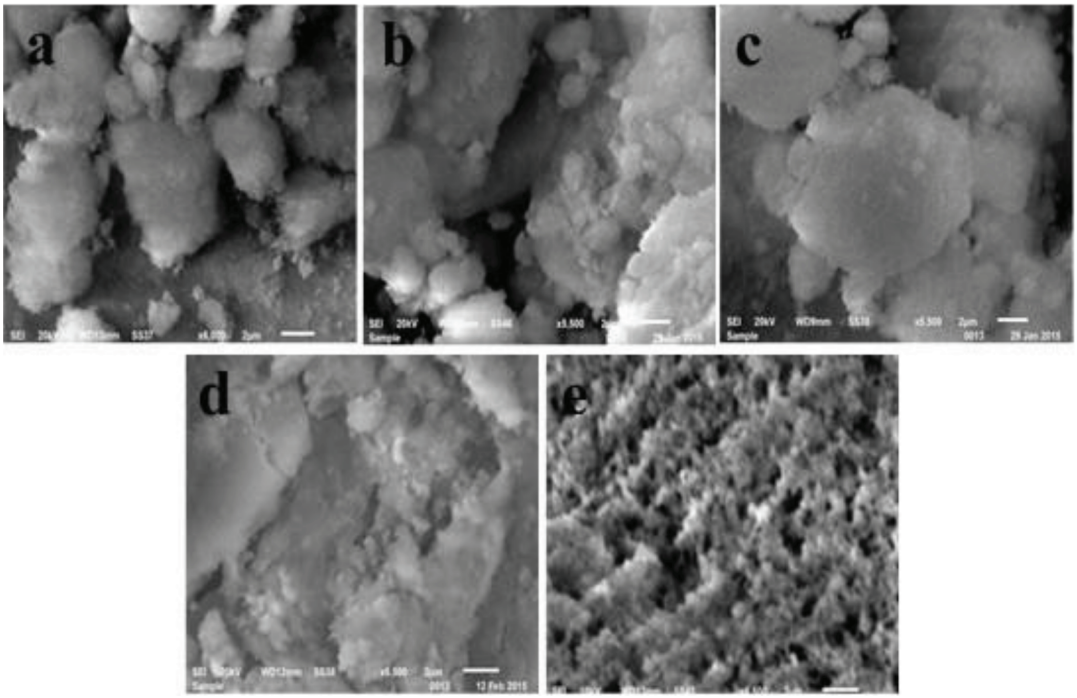

Figure 5. SEM micrographs of (a) HAP, (b) HAP/HPAM-0.75, (c) HAP/HPAM-3, (d) HAP/HPAM-30, and (e) HAP/HPAM-75 at 2 µm.

Table 3 presents the element's molar percentage and the final molar ratio Ca/P obtained by the EDS technique. For all materials, the obtained Ca/P values were inferior to the stoichiometric ratio of 1.67. According to the literature, Ca/P of less than 1.67 indicates the formation of highly calcium-deficient HAP.[27]. In our materials, the hydroxyapatite amounts contained in HAP and composites having a chemical formula similar to $Ca_{10}(PO_4)_{5.64}(CO_3)_{0.66}(OH)_{3.03}$ and $Ca_5(PO_4)_3(OH)$ were determined by XRD according to the mentioned PDF card.

Table 3. Surface composition of HAP and HAP/HPAM-n materials determined by EDS.

	Ca (%)	P (%)	O (%)	C (%)	N (%)	Ca/P
HAP	16.74	11.94	57.44	13.88	/	1.40
HAP/HPAM-0.75	17.10	13.10	54.50	15.30	/	1.30
HAP/HPAM-3	16.37	11.89	51.85	16.34	3.55	1.38
HAP/HPAM-30	13.26	10.01	48.17	25.51	3.05	1.32
HAP/HPAM-75	16.04	10.6	49.96	22.47	0.92	1.52

By comparison between the ratio of Ca/P in the two formulas (1.77 and 1.67) and the Ca/P ratio obtained by EDS, we deduce that the calcium atoms on the material's surface are covered by an excess of phosphate ions. The interior and the surface of materials thus do not have the same mineral structure.

In addition, it is known that HAP has a strong affinity for all kinds of molecules, including CO_2 and water. In consequence, we can estimate that the higher percentage of carbon found at the surface is not the real amount. As a conclusion from this part, the surface and the bottom of HAP and HAP/HPAM-n materials do not have the same mineral structure and the percentage of carbon is more important in the composite materials than in the HAP reference sample due to the presence of copolymer. The nitrogen atom of HPAM was also detected by EDS.

2.3. Methylene blue dye removal evaluation

2.3.1. Effect of HPAM initial amount on adsorption capacity

Each HAP/HPAM-n material was prepared with a determined amount of HPAM copolymer. The amount of MB adsorbed per gram of adsorbent as a function of the initial HPAM percentage in each HAP/HPAM-n was determined by batch method at 25 °C and pH 5.76. The adsorbent (20 mg) was added to 40 mL of dye solution with a concentration of 10 mg L^{-1}. The results obtained show that the adsorption capacity (qe) increases with increasing HPAM percentage. Thus, HAP, HAP/HPAM-0.75, HAP/HPAM-3, HAP/HPAMH-30, and HAP/HPAM-75 respectively show the following adsorption capacities (qe): 0.50 mg g^{-1}, 0.78 mg g^{-1}, 2.52 mg g^{-1}, 5.37 mg g^{-1}, and 10.95 mg g^{-1}. From these adsorption capacities, we see that the copolymer site is mainly responsible for the dye retention. The composites HAP/HPAM-30 and HAP/HPAM-75 are the best adsorbents for MB dye. These two materials swell in the MB dye aqueous solution, which makes the copolymer sites more accessible for the MB dye.

HAP/HPAM-75 composite was selected for dye adsorption evaluation because it is the material with the highest MB adsorption capacity. We must note that HPAM alone is not a candidate material for MB adsorption because it is soluble in colored aqueous solution. The value of qe is determined by Eq. (2):

$$qe = (C_0 - Ce)V/m, \tag{2}$$

where C_0 and Ce are the initial and equilibrium concentrations (mg L^{-1}) of MB, V is the volume of solution (mL), m is the weight of adsorbent (g) taken for the experiment, and qe is the adsorption capacity at equilibrium time (mg g^{-1}).

2.3.2. Contact time effect

The effect of contact time was studied using 40 mL of solution containing 10 mg L^{-1} concentration MB dye and 20 mg of each adsorbent for up to 360 min. Figure 6 shows that adsorption consisted of three distinct phases: the first phase lasted approximately 45 min, from 5 to 50 min. The q_t at 5 min is 11.72 mg g^{-1}, which indicates the spontaneous adsorption of MB on the material. Indeed, up to 50 min q_t attained a maximum at 20 min with 12.81 mg g^{-1}. From 20 to 50 min the adsorption capacity decreased. This phenomenon is explained by the swelling properties of the material and its porous structure, which lead to more trapped MB molecules. The second phase is from 50 min to 180 min. The behavior of MB adsorption on HAP/HPAM-75 in this phase is somewhat similar to the first one but with a low amount of desorbed MB. This is followed by the third phase, when a plateau is reached at 180 min. The best known models to investigate the sorption mechanism are the pseudo first-order and the pseudo second-order models. These models are defined respectively by Eqs. (3) and (4):

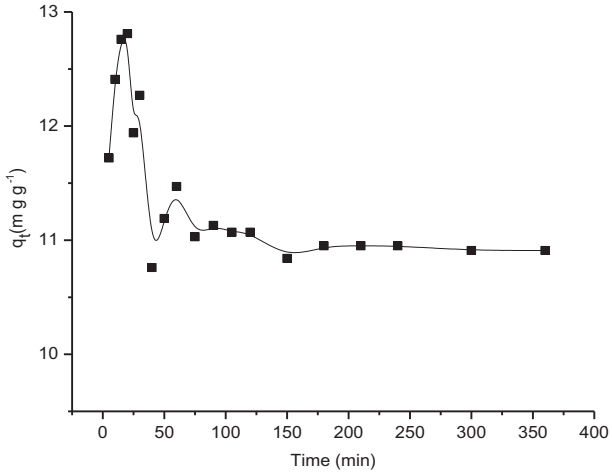

Figure 6. Time-dependent amount (q_t) of MB removed, [MB] = 10 mg L^{-1}, $m_{adsorbent}$ = 20 mg, V_{MB} = 40 mL, pH 5.76, T = 25 °C, 400 rpm.

$$\text{Pseudo first-order equation: } \log\ (q_e - q_t) = \log q_e - \frac{K_1}{2.303}\, t, \tag{3}$$

$$\text{Pseudo second-order equation: } \frac{t}{q_t} = \frac{1}{K_2 q_e^2} + \frac{1}{q_e} t, \tag{4}$$

where K_1 is the rate constant of pseudo first-order (min^{-1}), K_2 is the rate constant of pseudo second-order (g mg^{-1} min^{-1}), and q_t is the adsorption capacity at the determined time (mg g^{-1}).

K_1, K_2, and q_e values were calculated from the slopes and intercepts of the lines obtained by plotting log (q_e – q_t) against t and by plotting t / q_t against t. In our case, it is not possible to use the pseudo first-order to take the characteristic adsorption parameters because, before equilibrium, the majority of experimental points have q_t more important than q_t at equilibrium (10.95 mg g^{-1}); this makes q_e – q_t negative, and, as a consequence, it is not possible to use the logarithmic function. On the other hand, Figure 7 clearly shows that the linear plot of the pseudo second-order is a very good model for MB adsorption with a correlation degree square R^2 = 0.9999, rate constant K_2 = –5.06 × 10^{-2} g mg^{-1} min^{-1}, and theoretical q_e = 10.85 mg g^{-1}.

The obtained qe from the pseudo second-order is in agreement with the experimental value, which indicates that the model is good for MB adsorption.

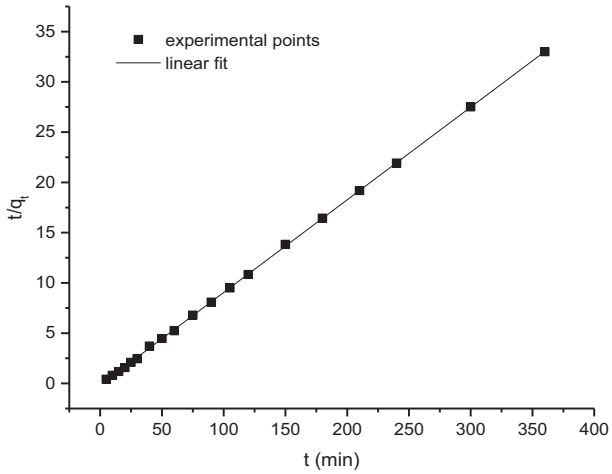

Figure 7. Linear fit of experimental data obtained using pseudo second-order, $R^2 = 0.999$.

2.3.3. Effect of MB concentration

Experiments were carried out on 20 mg of HAP/HPAM-75 at 25 °C and pH 5.76 for 3 h of contact time and using 40 mL of MB solution with various concentrations of the dye. The effect of initial dye concentration was investigated in the range of 5–500 mg L^{-1}. The MB adsorption capacity increased with increasing dye concentration from 5 mg L^{-1} to 300 mg L^{-1} and became constant at concentration above 300 mg L^{-1} with a maximum adsorption capacity (q_{max}) of 435.6 mg g^{-1}. The obtained q_{max} value indicates that HAP/HPAM-75 is a good candidate for MB removal from aqueous solution.

Adsorption isotherms are very useful, providing information on adsorption mechanisms, surface properties, and affinity of adsorbents towards adsorbates. To understand the mechanism, the experimental data were fitted to Langmuir, Freundlich, and Temkin adsorption models respectively using Eqs. (5), (6), and (7):

$$\text{Langmuir equation: } \frac{1}{q_e} = \frac{1}{K_1 q_{max} C_e} + \frac{1}{q_{max}}, \tag{5}$$

$$\text{Freundlich equation: } \log q_e = \log K_f + \frac{1}{n} \log C_e, \tag{6}$$

$$\text{Temkin equation: } q_e = \frac{RT}{b_t} \log a_t + \frac{RT}{b_t} \log C_e, \tag{7}$$

where K_l is the Langmuir constant (L mg^{-1}), q_{max} is the maximum adsorption capacity (mg g^{-1}), C_e is the concentration at equilibrium time (mg L^{-1}), K_f is the Freundlich constant (mg g^{-1}), n is the adsorption intensity, R is the ideal gas constant (8.314 J mol^{-1} K^{-1}), T is the temperature of study (K), and b_t (J mol^{-1}) and a_t (L mg^{-1}) are Temkin constants.

By plotting and fitting the different equations, we obtain correlation coefficients (R^2) of 0.583, 0.660, and 0.964 for the Langmuir, Freundlich, and Temkin models, respectively. From these values, we deduce that

adsorption of MB onto the HAP/HPAM-75 composite is defined by the Temkin model. The Langmuir and Freundlich models are not useful for our system, so it is not imperative to determine the parameters defined in Eqs. (5) and (6). From the Temkin model plotted in Figure 8, the characteristic constants are b_t equal to 6.61 J mol^{-1} and a_t equal to 0.23 L mg^{-1}. The applicability of the Temkin model indicates the interaction between the adsorbent and the adsorbate and the presence of MB–MB interaction as a consequence of the multilayer adsorption. The Temkin model also indicates the presence of electrostatic interaction between positive and negative charges.[14]

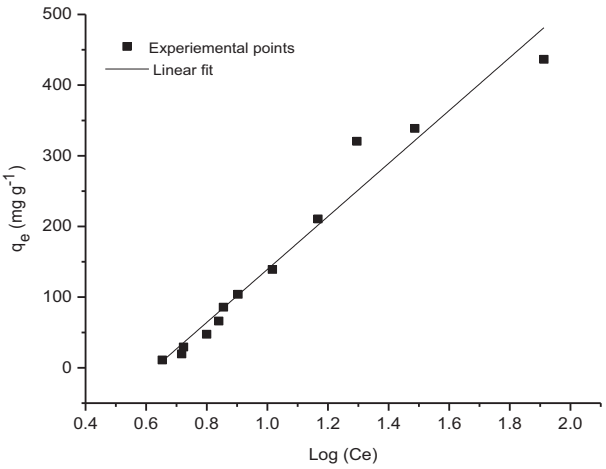

Figure 8. The experimental data fitting of Temkin model, $R^2 = 0.964$.

2.3.4. Effect of pH

pH is a very important parameter in adsorption process. Changing the pH can lead to a change in both adsorbent and adsorbate structures. The pH effect on MB removal by HAP and HAP/HPAM-75 at 25 °C was studied. The pH was varied between 4 and 10 by using HCl (1 mol L^{-1}) and NaOH (1 mol L^{-1}). The pH effect on MB retention is especially visible in this pH range. The HAP/HPAM-75 composite shows an increase in dye adsorption from 11.52 mg g^{-1} to 14.24 mg g^{-1}, contrary to the HAP material characterized by a very weak adsorption capacity from 0.5 mg g^{-1} to 0.95 mg g^{-1}. This increase is presented because the HAP part of the composite becomes negatively charged in alkaline medium. Corami et al.[6] reported that pH of zero charge is 7.4 for HAP material. Therefore, protonation–deprotonation of HAP is presented. Higher pH leads to a negative surface charge. On the other hand, lower pH leads to the protonation of HAP and the presence of positive charges. For this reason, qe is more important at higher pH. The possibility of hydrolyzing no linked amide groups to HAP phase in HAP/HPAM-75 is also possible; as a consequence, there is a significant increase in the adsorbed quantity of dye in comparison to HAP alone.

2.3.5. Temperature effect

The temperature effect on MB retention by HAP/HPAM-75 reveals that removed quantity decreases with increasing temperature. The enthalpy change (ΔH) and entropy change (ΔS) were calculated by using the

van't Hoff equation in the following form:

$$\ln K_c = \frac{\Delta S}{R} - \frac{\Delta H}{RT}, \tag{8}$$

where K_c is the equilibrium constant equivalent to the fractional attainment of MB adsorbed onto HAP/HPAM-75. K_c is calculated according to Eq. (9):

$$K_c = \frac{C_0 - C_e}{C_e}, \tag{9}$$

where C_0 and Ce are the initial and equilibrium concentrations of MB, respectively (mg L^{-1}); T is the temperature (K); and R is the ideal gas constant (8.314 J mol^{-1} K^{-1}). Values of ΔH and ΔS were calculated from the slope and intercept of lnKc as a function (1000 / T) plot (Figure 9). The values of thermodynamic parameters ΔH, ΔS, and Gibbs free energy (ΔG) are given in Table 4, where ΔG values are determined at each temperature by using Eq. (10):

$$\Delta G = \Delta H - T\Delta S. \tag{10}$$

The negative value of ΔH shows that adsorption of MB on HAP/HPAM-75 is an exothermic process. The negative value of ΔS indicates that the randomness decreases at the solid–solution interface during the adsorption of dye on the composite. In addition, ΔG becomes positive when the temperature rises, indicating that the MB adsorption phenomenon is not favorable at high temperatures.

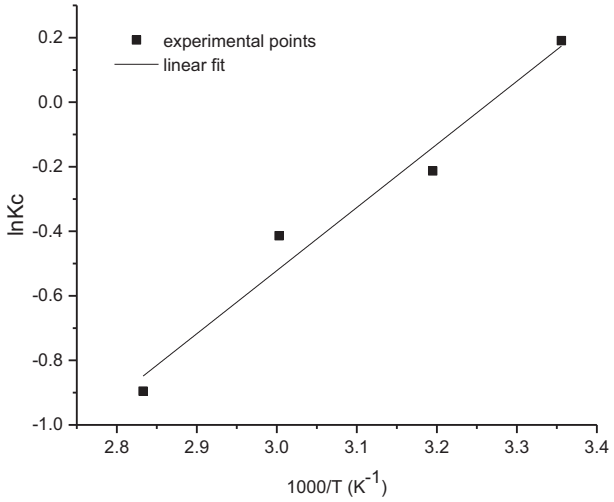

Figure 9. The van't Hoff plot of the adsorption of MB onto HAP/HPAM-75, [MB] = 10 mg L^{-1}, $m_{adsorbent}$ = 20 mg, V_{MB} = 40 mL, t_{eq} = 3 h, pH 5.76, 400 rpm, R^2 = 0.970.

Table 4. Thermodynamic parameters for adsorption of MB onto HAP/HPAM-75 composite at pH 5.76, t_{eq} = 3 h, [MB] = 10 mg L^{-1}, $m_{adsorbent}$ = 20 mg, V_{MB} = 40 mL, 400 rpm.

Sample	ΔH (kJ mol^{-1})	ΔS (J mol^{-1} K^{-1})	ΔG (kJ mol^{-1})				R^2
			298 K	313 K	333 K	353 K	
HAP/HPAM-75	–16.25	–53.11	-0.42	0.37	1.43	2.50	0.970

2.3.6. Composite reuse

The reuse or regeneration ability for each adsorbent is an important property. It minimizes the cost of the adsorption process with the possibility to reuse the adsorbent several times. Many reagents for MB desorption from different adsorbents are reported in the literature, such as ethanol, acetic acid, HCl, KCl, and phosphoric acid.[16,28–31]

In order to study the regeneration of HAP/HPAM-75, a fixed mass of adsorbent was added to a fixed volume of MB dye having a concentration of 10 mg L^{-1} in order to obtain a ratio between the mass of adsorbent and volume of dye equal to 1 mg mL^{-1}. Three regeneration cycles were realized.

HAP/HPAM-75 after adsorption of dye was placed in a minimum volume of hydrochloric acid at pH 4 and stirred for 3 h. The solids were filtered and placed in a minimum volume of absolute ethanol, then stirred to observe the white color of the powder, which indicates a complete desorption of adsorbed dye molecules.

The white powder was filtrated from ethanol solution, washed with double-distilled water, and dried at 60 °C for 40 min, then placed again in MB solution retaining the experimental conditions of equilibrium time, temperature, pH, stirring speed, and dye concentration.

After 3 h, as equilibrium time, the regenerated material was separated from the MB solution and the supernatant was analyzed by UV-Vis spectrophotometer. The same experiment was repeated to obtain three regeneration cycles. For each cycle, we determined the percentage of adsorption efficiency (ads (%)) as expressed in Eq. (11). For HAP/HPAM-75, the determined percentages are 78.72%, 72.88%, and 72.26%, corresponding respectively to the regeneration cycles from the first cycle to the third one. A small decrease in adsorption efficiency was observed but, in general, both materials have percentages higher than 70%. This result indicates that HAP/HPAM-75 is a good material for MB dye removal from aqueous solution with good recyclable properties.

$$ads\ (\%) = \frac{C_0 - C_e}{C_0} 100, \tag{11}$$

where C_0 and Ce are the initial and the equilibrium dye concentrations, respectively.

2.4. Conclusions

The in situ method is an effective route to prepare composites based on hydroxyapatite and soluble copolymer as partially hydrolyzed HPAM. The XRD technique of the obtained materials confirms that HAP was formed within the copolymer and reveals that functional groups of HPAM are incorporated in the crystalline lattice of hydroxyapatite. On the other hand, the morphology of HAP/HPAM-n materials is also different. The HAP without copolymer is largely agglomerate, but the HAP/HPAM-0.75, HAP/HPAM-3, and HAP/HPAM-30 composites are more agglomerate and the materials are highly recovered with copolymer.

The study of HPAM amount effect on the composite interactions with a cationic molecule such as MB reveals a remarkable amelioration in the retention efficiency. This result encouraged us to study the adsorption parameters and to show that the dye retention on HAP/HPAM-75 is defined by the Temkin model with an exothermic and spontaneous process. The regeneration ability of the material also confirms that the composite HAP/HPAM-75 is a high-performance recyclable adsorbent and it is a good candidate for MB cationic dye removal.

3. Experimental

3.1. Reagents

Hydrochloric acid, MB, and sodium hydroxide were supplied by Sigma-Aldrich Company. Absolute ethanol was purchased from Biochem Chemopharma. The calcium source was prepared in our laboratory from calcium carbonate and contained 80% calcium hydroxide. Its composition was determined by TGA. Phosphoric acid (85%) was supplied by Sigma-Aldrich Company. The partially hydrolyzed HPAM, also known as AD37 copolymer, was provided by Rhône-Poulenc Company (France). Its weight-average molar mass was estimated by viscosity technique and confirmed by light scattering to be 2.48×10^6 g mol^{-1}. The hydrolyzed carboxylate rate of HPAM is about 27%, conferring high water solubility explained by the negative charges on the copolymer backbone.

3.2. Sample characterizations

The synthesized powders were characterized using the XRD Rigaku IV (LAEPO Laboratory, University of Tlemcen) with CuKα irradiation at 1.54 Å using 2 theta (2θ) = 0.02°in the range of 3°to 70°. XRD was used to investigate the formation of HAP in the presence of HPAM and to evaluate their effect on the crystalline aspect of the synthesized composites.

Infrared spectra were recorded on the FTIR Agilent Technologies Cary 600 Series with a resolution of 4 cm^{-1}. They were used to observe the characteristic transmittance bands in HAP/HPAM-n. Morphology observations and percentage elements surface determination were performed using a JEOL JED-2300 scanning electron microscope instrument coupled with SEM/EDS. The TGA TA SDT Q600 (LAEPO-Laboratory, University of Tlemcen) was used to study the thermal behavior and stability of HAP and HAP/HPAM-n and to determine the HPAM copolymer weight loss of the different composites.

3.3. Sample preparation

In order to obtain HAP/HPAM-n composites, HAP was prepared via in situ chemical wet precipitation in the HPAM medium with stoichiometric initial molar ratio of calcium/phosphate (Ca/P) = 1.67. The HPAM structure is represented in Figure 10 and the chemical equation describing the reaction is as follows:

$$8Ca(OH)_2 + 2CaCO_3 + 6H_3PO_4 + HPAM \rightarrow Ca_{10}(PO_4)_6(OH)_2/HPAM + 16H_2O + 2CO_2 \qquad (12)$$

The precipitation was performed by preparing a water suspension of calcium. For this purpose, 0.067 mol calcium was dispersed in the HPAM aqueous solution having the desired copolymer concentration. The mixture was stirred for 24 h. Then 0.04 mol phosphoric acid H_3PO_4 solution was added dropwise at a rate of 2 mL min^{-1} to the calcium suspension. Initial pH was basic and indicated the liberation of hydroxyl groups from $Ca(OH)_2$ during the synthesis. The basic pH medium is important for HAP formation and it implies the dissociation of H_3PO_4 to PO_4^{3-}. The calcium phosphate formed as phosphoric acid was added and the mixture was stirred at 750 rpm speed for 24 h at ambient temperature and atmospheric pressure. The mixture was filtered and dried at 70 °C for 12 h. The obtained powders, summarized in Table 5, were named HAP and HAP/HPAM-n, with n being the weight percentage of HPAM to HAP, equal to 0.75%, 3%, 30%, and 75%.

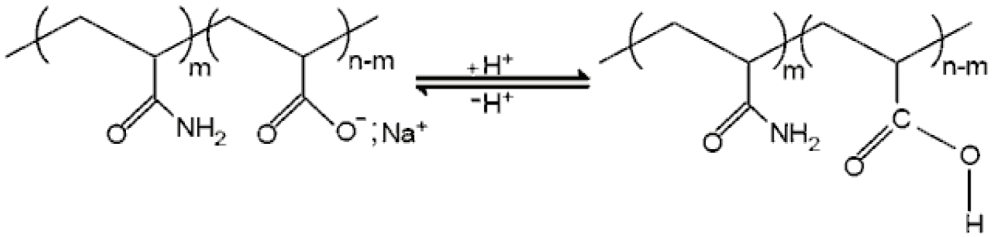

Figure 10. Chemical structure of partially hydrolyzed polyacrylamide (HPAM).

Table 5. Preparation of HAP/HPAM-n powders from different HPAM concentrations. *Initial ratio of HPAM to calcium source (m_p/m_{Ca}), **initial ratio of HPAM to HAP (m_p/m_{HAP}), ***initial ratio of HPAM to composite (m_p/m_{comp}) (m_{comp} is both HPAM and HAP mineral).

	[HPAM] gL^{-1}	m_p/m_{Ca}* (%)	m_p/m_{HAP}** (%)	m_p/m^{***}_{comp} (%)
HAP/HPAM-0.75	0.25	1	0.75	0.7
HAP/HPAM-3	1	4	3	2.85
HAP/HPAM-30	10	40	30	22.3
HAP/HPAM-75	25	100	75	42

3.4. Dye solution preparation and adsorption experiments

MB is a cationic dye. Its chemical formula is $C_{16}H_{18}N_3SCl$ and its molecular weight is 319.85 g mol^{-1}. Dye solution was prepared by dissolving 2 g of dye in 1L of bidistilled water to obtain a stock solution. All other concentrations were obtained by diluting the stock solution and 20 mg of each adsorbent was added to 40 mL of MB solution to obtain the desired concentration. The adsorbate and adsorbent were agitated at 400 rpm using a magnetic stirrer. The samples from the solution were separated by centrifugation using a Hettich UNIVERSAL 23 R centrifuge apparatus (LAEPO-Laboratory, University of Tlemcen).

It is not imperative to use centrifugation for HAP/HPAM-30 and HAP/HPAM-75 because the composites separate at once from the dye solution as a consequence of hydrophobic properties. The dye solution concentration was determined by using a UV OPTIZEIN 1412V-FB UV-Vis spectrophotometer (LAEPO-Laboratory, University of Tlemcen) at the maximal absorption wavelength of 664 nm.

References

1. Malmberg, P.; Nygren, H. *Proteomics* **2008**, *8*, 3755-3762.
2. Batchelar, D. L.; Davidson, M. T. M.; Dabrowski, W.; Cunningham I. A. *Med. Phys.* **2006**, *33*, 904-915.
3. Yang, C. C.; Li, Y. J.; Chiu, S. J.; Lee, K. T.; Chien, W. C.; Huang, C. A. *J. Power Sources* **2008**, *184*, 95-98.
4. Jungbauer, A.; Hahn, R.; Deinhofer, K.; Luo, P. *Biotechnol. Bioeng.* **2004**, *87*, 364-375.
5. Gupta, N.; Kushwaha, A.; Chattopadhyaya, M. C. *J. Taiwan. Inst. Chem. E* **2012**, *43*, 125-131.
6. Corami, A.; Mignardi, S.; Ferrini, V. *J. Colloid. Interface. Sci.* **2008**, *317*, 402-408.
7. Lin, K.; Pan, J.; Chen, Y.; Cheng, R.; Xu, X. *J. Hazard. Mater.* **2009**, *161*, 231-240.
8. El-Zahhar, A. A.; Awwad, N. S. *J. Environ. Chem. Eng.* **2016**, *4*, 633-638.
9. Hakimimehr, D.; Liu, D. M.; Troczynski, T. *Biomaterials* **2005**, *26*, 7297-7303.
10. El-Hag Ali, A. *J. Macromol. Sci. A* **2012**, *49*, 7-14.

11. Syusyukina, V. A.; Shapovalova, Y.; Korotchenko, N. M.; Kurzina, I. A. *Russ. J. Appl. Chem.* **2017**, *90*, 106-112.
12. Baybas, D.; Ulusoy, U. *J. Solid. State. Chem.* **2012**, *194*, 1-8.
13. Yokoi, T.; Kawashita, M.; Kikuta, K.; Ohtsuki, C. *Mater. Sci. Eng. C* **2010**, *30*, 154-159.
14. Liao, N.; Liu, Z.; Zhang, W.; Gong, S.; Ren, D.; Ke, L.; Lin, K.; Yang, H.; He, F.; Jiang, H. *J. Macromol. Sci. A* **2016**, *53*, 276-281.
15. Baybaş, D.; Ulusoy, U. *Turk. J. Chem.* **2014**, *40*, 147-162.
16. Meral, K.; Metin, O. *Turk. J. Chem.* **2014**, *38*, 775-782.
17. Yang, G.; Zhang, L.; Peng, T.; Zhong, W. *J. Membr. Sci.* **2000**, *175*, 53-60.
18. Ninan, N.; Muthiah, M.; Park, I. K.; Elain, A.; Thomas, S.; Grohens, Y. *Carbohydr. Polym.* **2013**, *98*, 877-885.
19. Shen, X.; Shamshina, J. L.; Berton, P.; Gurauc, G.; Robin R. D. *Green Chem.* **2016**, *18*, 53-75.
20. Wang, Q. G.; Wimpenny, I.; Dey, R. E.; Zhong, X.; Youle, P. J.; Downes, S.; Watts, D. C.; Budd, P. M.; Hoyland, J.A.; Gough, J. E. *J. Biomed. Mater. Res. A* **2018**, *106*, 168-179.
21. Mansri, A.; Tennouga, L.; Desbrières, J. *Eur. Polym. J.* **2007**, *43*, 540-549.
22. Mansri, A.; Tennouga, L.; Bouras, B. *J. Mater. Environ. Sci.* **2014**, *5*, 37-42.
23. Varma, H. K.; Babu, S. S. *Ceram. Int.* **2005**, *31*, 109-114.
24. Balamurugan, A.; Michel, J.; Fauré, J.; Benhayoune, H.; Wortham, L.; Sockalingum, G.; Banchet, V.; Bouthors, S.; Laurent-Maquin, D.; Balossier, G. *Ceram. Silikaty* **2006**, *50*, 27-31.
25. Zhu, D.; Wei, L.; Wang, B.; Feng, Y. *Energies* **2014**, *7*, 3858-3871.
26. Chenxin, X.; Yujun, F.; Weiping, C.; Houkai, T.; Jufeng, L.; Zhiyong, L. *J. Appl. Polym. Sci.* **2009**, *111*, 2527-2536.
27. Sadat-Shojai, M.; Khorasani, M. T.; Jamshidi, A. *J. Cryst. Growth* **2012**, *361*, 73-84.
28. Wei, W.; Yang, L.; Zhong, W. H.; Li, S.Y.; Cui, J.; Wei, Z. G. *Dig. J. Nanomater. Bios.* **2015**, *10*, 1343-1363.
29. Sajab, M. S.; Chia, C. H.; Zakaria, S.; Jani, S. M.; Ayob, M. K.; Chee, K. L.; Khiew, P. S.; Chiu, W. S. *Bioresource. Technol.* **2011**, *102*, 7237-7243.
30. Saber-Samari, S.; Saber-Samari, S.; Nezafati, N. ; Yahya, K. *J. Environ. Manag.* **2014**, *146*, 481-490.
31. Chen, R. P.; Zhang, Y. L.; Wang, X. Y.; Zhu, C. Y.; Ma, A. J.; Jiang, W. M. *Desal. Water. Treat.* **2015**, *55*, 539-548.